Raman Spectroscopy of the Filamentous Virus *Ff* (*fd, f1, M13*): Structural Interpretation for Coat Protein Aromatics[†,‡]

Stacy A. Overman and George J. Thomas, Jr.*

Division of Cell Biology and Biophysics, School of Biological Sciences, University of Missouri−Kansas City, Kansas City, Missouri 64110

Received November 30, 1994; Revised Manuscript Received February 24, 1995[⊗]

ABSTRACT: Site-specific isotope substitutions in the coat protein (pVIII) of the filamentous bacterial virus *Ff* (*fd, f1, M13*) have been employed to advance vibrational band assignments and facilitate structural interpretation of the Raman spectrum. We report spectra of phage *fd* assembled *in vivo* from pVIII subunits incorporating either deuteriophenylalanine (F_{d5}), deuteriotryptophan (W_{d5}), or deuteriotyrosine (Y_{d4}) residues with labeled ring sites. The deuterated aromatics were introduced into *fd* individually and in combination. On the basis of observed isotope shifts, definitive assignments have been developed for all prominent Raman bands diagnostic of the pVIII aromatic residues (F11, F42, F45, W26, Y21, Y24). The present study constitutes the first direct experimental determination of Raman fingerprints of tyrosine and phenylalanine side chains within hydrophobic α-helical domains and yields unexpected results. Importantly, neither Y21 nor Y24 of pVIII exhibits the "canonical" Fermi doublet expected in the 820−860 cm^{-1} interval of the Raman spectrum. Instead, each tyrosine exhibits a single band near 853 cm^{-1}. Since the application of denaturing conditions is sufficient to generate in *fd* an apparent Fermi doublet, it is concluded that the anomalous singlet is intrinsic to tyrosine environments in the native virion assembly. In addition, the Raman results clearly demonstrate an interdependence of the environments of aromatic side chains in virion subunits. We show that the results on *fd* isotopomers are also confirmed by Raman spectroscopy of *Ff* virions incorporating the tyrosine mutations Y21M, Y24M, and Y21F/Y24S. The Raman marker bands identified for pVIII aromatics modify and extend Raman correlations proposed previously for proteins. The unusual environments detected for aromatic residues in the mature *Ff* assembly are discussed in relation to recently proposed models for filamentous virion architecture.

Ff[1] is the class prototype of long (≈880 nm) and thin (≈7 nm diameter) bacterial viruses infecting F^+ strains of *Escherichia coli*. The filamentous phages *fd*, *f1*, and *M13* are structurally similar members of the *Ff* class, in which a single-stranded DNA loop of about 6410 nucleotides is packaged within a sheath of several thousand copies of a 50-residue subunit, the product of viral gene VIII. The pVIII subunits constitute about 87% of the total virion mass. The pVIII sequence ([1]AEGDDPAKAAFDSLQASATEYIGY-AWAMVVVIVGATIGIKLFKKFTSKAS[50]) is identical in subunits of *fd* and *f1* virions and differs by only a single residue (N12) in the subunit of *M13*. The uses of *Ff* as a cloning vector, as a vehicle for antigen display, and as a paradigm of nucleoprotein assembly within a membrane bilayer have combined to make the virion, and especially its pVIII subunit, a target of structural analysis by diffraction and spectroscopic methods. Further details of the molecular genetics, architecture, and assembly of the *Ff* virus are given in the monograph edited by Denhardt et al. (Denhardt et al., 1978) and in recent reviews (Webster & Lopez, 1985; Model & Russel, 1988; Russel, 1991; Opella & McDonnell, 1993; Miura & Thomas, 1994) and journal articles (Aubrey & Thomas, 1991; Glucksman et al., 1992; McDonnell et al., 1993; Marvin et al., 1994).

The large body of structural work on *Ff*, including studies by fiber X-ray and neutron diffraction (Glucksman et al., 1992; Marvin et al., 1994), solid-state NMR spectroscopy (Cross et al., 1983; McDonnell et al., 1993), solution Raman spectrosopy (Thomas & Murphy, 1975; Thomas et al., 1983; Overman et al., 1994), and CD spectroscopy (Clack & Gray, 1989; Arnold et al., 1992), indicate a uniformly α-helical secondary structure for the pVIII subunit in the native virus. Close packing of pVIII α-helices is generally assumed in proposed molecular models (Marvin, 1990; Glucksman et al., 1992; Marvin et al., 1994). However, experimental evidence delineating side-chain environments is scant, and knowledge of the specific side-chain interactions which stabilize subunit packing in the native *Ff* assembly is very limited (Gall et al., 1982; Thomas et al., 1983; Aubrey & Thomas, 1991; Arnold et al., 1992). More detailed information regarding the pVIII side-chain environments is required in order to accurately model protein−protein and protein−DNA interfaces in the *Ff* assembly. This information is also

[†] Support of this research by the National Institutes of Health (Grant GM 50776) is gratefully acknowledged.

[‡] Part 45 in the series Studies of Virus Structure by Laser Raman Spectroscopy.

* To whom correspondence may be addressed.

[⊗] Abstract published in *Advance ACS Abstracts,* April 1, 1995.

[1] The *Ff* coat protein is the product of viral gene VIII, designated pVIII. A pVIII amino acid residue and its sequence position are indicated by a one-letter abbreviation and numeral in roman type. For example, Y21 denotes tyrosine at position 21; Y21M denotes the mutation of Y21 to methionine. Deuterium substituents on aromatic amino acid rings are indicated by subscripts. For example, Y_{d4} denotes tetradeuteriated tyrosine; *fd*($2Y_{d4}$) denotes phage containing two tetradeuteriotyrosines per coat protein. Normal modes of vibration for aromatic residues are indicated by italic type. For example, *Y1* denotes normal mode 1 of tyrosine (Harada & Takeuchi, 1986). Normal mode designations for other protein aromatics are given by Austin et al. (1993) and references therein.

0006-2960/95/0434-5440$09.00/0

expected to provide a better understanding of pVIII polymorphism and its relevance to proposed assembly and disassembly mechanisms (Marvin, 1989; Shon et al., 1991; Nambudripad et al., 1991; McDonnell et al., 1993).

Raman spectroscopy has been applied extensively as a structural probe of *Ff* viruses. Yet, only a fraction of the potentially informative Raman bands has so far been exploited for structural conclusions. A major reason is the prerequisite for unambiguous Raman band assignments. The number of definitive assignments can be advanced by comparisons with model compounds of known Raman signature, and especially by the introduction of residue-specific modifications which perturb vibrational dynamics in a predictable manner without altering the conformations or assembly characteristics of viral components. Accordingly, isotope substitution is the method of choice for advancing Raman spectral assignments and promoting structural conclusions therefrom. Previously, we utilized this approach through *in vivo* incorporation of deuterioalanine and deuteriotryptophan into coat proteins of phage *fd* (Aubrey & Thomas, 1991).

In the present work we extend the systematic assignment of all bands in the *Ff* Raman spectrum by analysis of isotopic derivatives (isotopomers) of *Ff* comprising pVIII subunits in which the aromatic protons of phenylalanine and tyrosine residues have been replaced by deuterium. We also report new results on the *Ff* isotopomer containing deuterium substitution of indole ring protons. The pVIII aromatics generate the most abundant and most intense contributions to the *Ff* Raman spectrum, and the vibrational origins of most of these bands are reasonably well understood [reviewed in Harada and Takeuchi (1986) and Austin et al. (1993)]. In combination with results reported previously for alanine and tryptophan isotopomers of *Ff* (Aubrey & Thomas, 1991), the present data provide comprehensive assignments for the more than 60 bands in the Raman spectrum of *Ff* which originate from the pVIII aromatic side chains (residues F11, Y21, Y24, W26, F42, and F45). The location of tyrosine and tryptophan side chains in the hydrophobic domain at the center of the pVIII sequence and the probable clustering of aromatics of neighboring subunits (Glucksman et al., 1992; Marvin et al., 1994) contribute to interest in their Raman signatures and roles in assembly.

The specific isotopomers examined here and the nomenclature employed are as follows: (i) *fd*($3F_{d5}$) represents the virion incorporating L-phenylalanine-2′-L-phenylalanine-2′,3′,4′,5′,6′-*d*5 (F_{d5}) at positions F11, F42, and F45 in the pVIII sequence; (ii) *fd*(W_{d5}) incorporates L-tryptophan-2′-L-tryptophan-2′,4′,5′,6′,7′-*d*5 (W_{d5}) at W26; (iii) *fd*($2Y_{d4}$) incorporates L-tyrosine-2′-L-tyrosine-2′,3′,5′,6′-*d*4 (Y_{d4}) at Y21 and Y24; and (iv) *fd*($3F_{d5}$,W_{d5},$2Y_{d4}$) incorporates F_{d5} at F11, F42, and F45, W_{d5} at W26, and Y_{d4} at Y21 and Y24. Raman spectra of these *fd* isotopomers are augmented by data from mutant *f1* virions containing site-specific mutations of one or both pVIII tyrosines. The mutants are designated as *f1*(Y21M), *f1*(Y24M), and *f1*(Y21F/Y24S), and a preliminary analysis of the distinctive spectral characteristics of these mutants has been given recently (Overman et al., 1994). Interpretation of the Raman spectra is facilitated by use of digital difference methods which permit accurate comparison of spectral intensities in wild-type, mutant, and deuterated *Ff* virions.

The direct methods employed here provide the most reliable and comprehensive approach to definitive Raman band assignments for filamentous viruses. The results obtained have been exploited to reach new structural conclusions about the *Ff* filament, including identification of novel molecular environments for subunit tyrosines in the assembled virion. Additionally, the large body of data collected on *Ff* isotopomers reveals numerous heretofore unrecognized Raman bands of protein aromatic side chains. These aromatic markers are an important supplement to existing spectra−structure correlations (Siamwiza et al., 1975; Miura et al., 1988, 1989; Harada et al., 1986; Takeuchi et al., 1989) and are expected to be useful in future structural studies of proteins and nucleoprotein assemblies by Raman spectroscopy.

EXPERIMENTAL PROCEDURES

Preparation and Purification of Viruses: Deuterations and Mutations of pVIII Side Chains. Deuterated amino acids L-phenylalanine-2′-L-phenylalanine-2′,3′,4′,5′,6′-*d*5 (F_{d5}), L-tryptophan-2′-L-tryptophan-2′,4′,5′,6′,7′-*d*5 (W_{d5}), and L-tyrosine-2′-L-tyrosine-2′,3′,5′,6′-*d*4 (Y_{d4}) were obtained from Cambridge Isotope Laboratories (Woburn, MA). Normal amino acids, growth media, and standard reagents were obtained from Sigma Chemical Company (St. Louis, MO) and Fisher Scientific (St. Louis, MO). Solution spectra of the aromatic amino acids are shown in Figure 1.

Normal *fd* and its aromatic isotopomers [designated *fd*($3F_{d5}$), *fd*(W_{d5}), *fd*($2Y_{d4}$), and *fd*($3F_{d5}$,W_{d5},$2Y_{d4}$)] were grown on *Escherichia coli* strain Hfr3300, obtained from Dr. Loren A. Day, Public Health Research Institute, New York, NY. The derivative *fd*($3F_{d5}$) was also grown on *E. coli* strain AT2471, a tyrosine auxotroph obtained from the *E. coli* Genetic Stock Center (CGSC stock no. 4510), courtesy of Prof. Barbara Bachman, Department of Biology, Yale University, New Haven, CT (Taylor & Trotter, 1967). Wild-type and mutant *f1* phages were the gift of Prof. Gianni Cesareni, Dipartimento di Biologia, Universita di Roma, Rome, Italy. Mutants replacing the coat protein tyrosines singly [*f1*(Y21M) and *f1*(Y24M)] and in combination [*f1*(Y21F/Y24S)] were constructed by site-directed mutagenesis, as detailed previously (Overman et al., 1994).

Normal phage were grown in MS media. To incorporate deuterated amino acids into the coat protein of *fd*, the host and phage were grown in M9 minimal media containing the appropriate deuterium-labeled L-amino acid at 0.1 mM per pVIII residue. The media also contained each remaining L-amino acid at 0.1 mM, 10 μg/mL thiamine−HCl, and 1% glucose. Similar methods have been employed to label *fd* protomers for solid-state NMR analysis (Cross et al., 1983). Mature viral particles, extruded through the bacterial cell membrane and into the growth media, were collected by precipitation with poly(ethylene glycol) (20 g/L) and NaCl (0.5 M) followed by low-speed centrifugation. The solid was resuspended in 10 mM Tris (pH 7.8), and the resulting solution was purified on a continuous KBr gradient (1.257 g/mL) in a Beckman SW41 rotor (Beckman Instruments, Fullerton, CA) at 38 000 rpm for 48 h at 4 °C. The phage band was collected, diluted 2-fold with 10 mM Tris, and subjected to four cycles of centrifugation in a Beckman Ti50 rotor at 40 000 rpm for 2 h at 4 °C followed by resuspension of the pellet in 10 mM Tris buffer. This procedure accomplishes essentially complete removal of excess KBr and produces the low-salt form of the virus as characterized previously (Thomas et al., 1983). Mutant phages *f1*(Y21M),

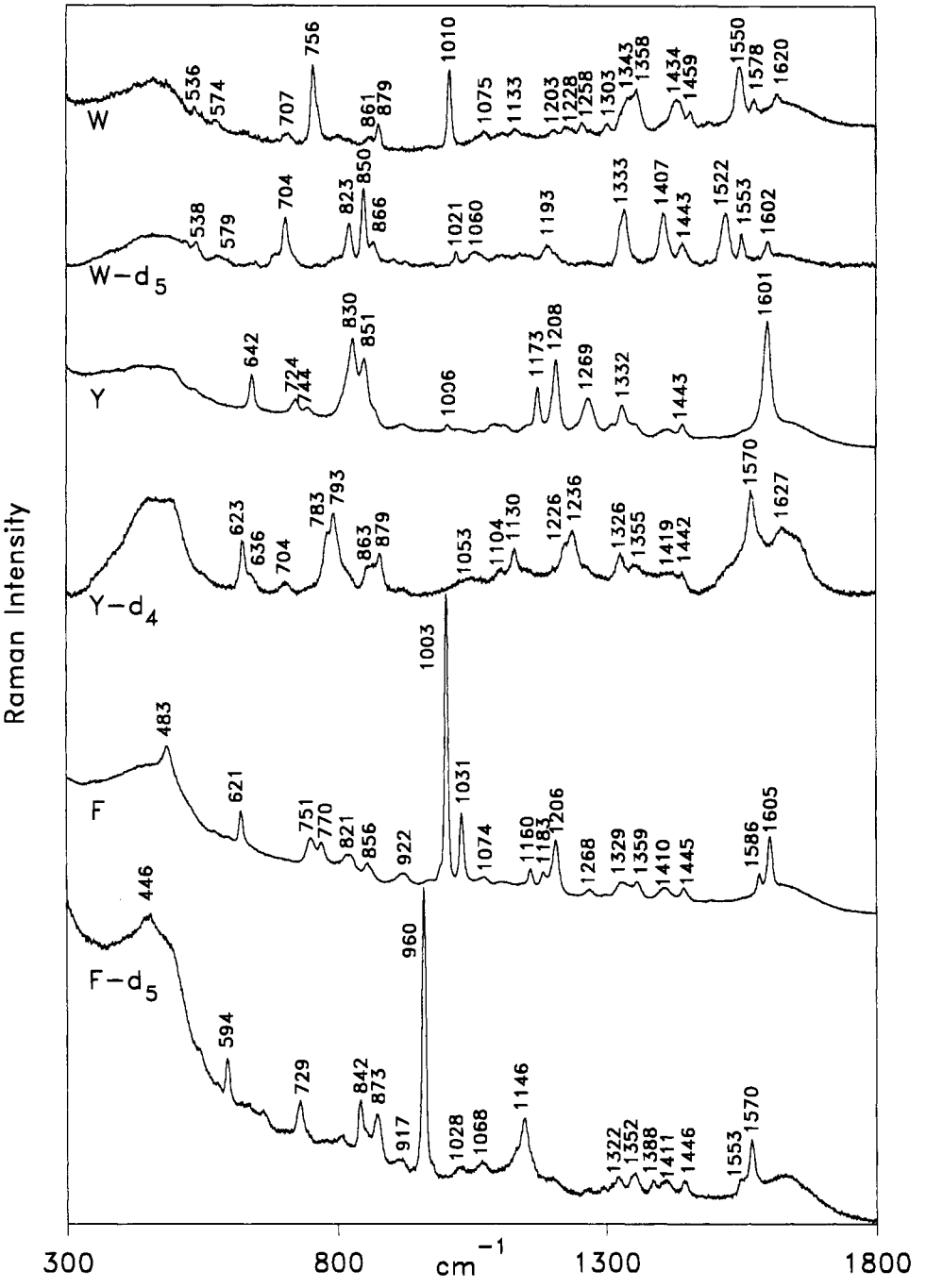

FIGURE 1: Raman spectra in the 300−1800 cm^{-1} region of normal (unlabeled) and deuterated aromatic amino acids. Frequencies of prominent bands are indicated in wavenumber units (cm^{-1}). Each amino acid was dissolved to saturation (≈50−100 mg/mL) in H_2O at pH 7.0 (phenylalanine and tryptophan) or pH 11.4 (tyrosine). Conditions: Excitation wavelength, 514.5 nm; laser power, 400 mW; sample temperature, 12 °C; spectral slit width, 8 cm^{-1}; increment, 1 cm^{-1}; integration time, 1.5 s. Each spectrum is the average of two scans. No smoothing or solvent corrections were employed.

f1(Y24M), and *f1*(Y21F/Y24S) were prepared, isolated, and purified similarly, as described by Overman et al. (1994). Typically, 20−40 mg of purified phage particles was obtained from a 1-L preparation. Purified virus preparations were stored at 4 °C prior to collection of Raman spectra.

The extent of incorporation of specifically deuterated amino acids was assayed by Raman spectrophotometric analysis, as described (Aubrey & Thomas, 1991). At least 99% incorporation of deuterium labels was achieved in each case. Isotopic purity is clearly illustrated for the case of *fd*($3F_{d5}$) in Figure 2. Here, the characteristic Raman marker of the phenylalanine ring at 1002 cm^{-1} in the spectrum of normal *fd* is essentially completely eliminated from the spectrum of *fd*($3F_{d5}$). The latter exhibits instead the distinctive marker of the deuteriophenyl ring at 960 cm^{-1}.

Raman Spectroscopy. Solutions of viruses (≈80 mg/mL, pH 7.8 ± 0.2) and amino acids (≈50−100 mg/mL) were sealed in standard glass capillaries (KIMAX No. 34507) for Raman analysis. Typically, a 2-μL aliquot was sufficient to fill the portion of the sample cell exposed to laser illumination. All spectral data were collected from samples thermostated at 12 °C (Thomas & Barylski, 1970).

Raman spectra were excited at 514.5 nm using an argon laser (Innova 70, Coherent Inc., Santa Clara, CA) of 400 mW radiant power at the sample cell, and were recorded on a computer-controlled scanning double spectrometer (Ra-

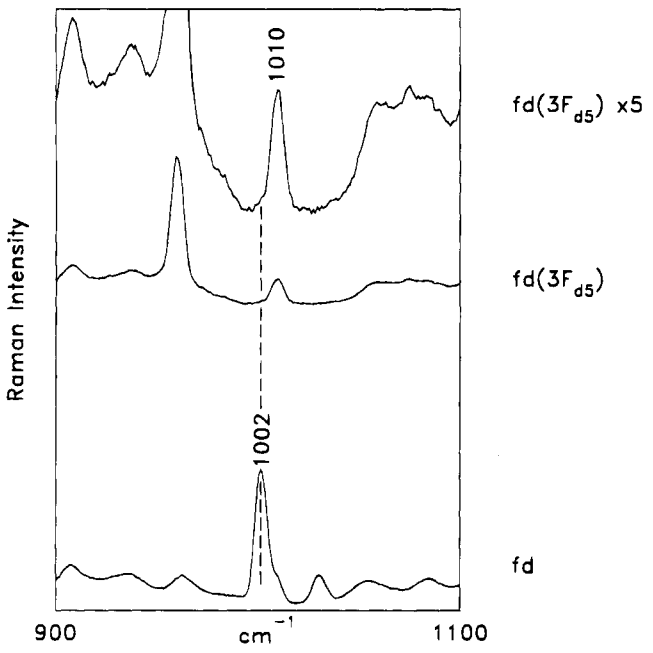

FIGURE 2: Raman spectra (900−1100 cm^{-1}) of unlabeled *fd* (bottom) and *fd*(3F$_{d5}$) (middle), showing elimination of the characteristic phenyl ring mode at 1002 cm^{-1} upon F$_{d5}$ incorporation. The residual intensity at 1002 cm^{-1} in the amplified spectrum of *fd*(3F$_{d5}$) (top) indicates <2% unlabeled *fd*. Virus concentration is 80 mg/mL in 10 mM Tris at pH 7.8. Each spectrum is the average of eight scans. Other conditions are given in Figure 1.

malog V/VI, Spex Inds., Edison, NJ) equipped with a photon-counting detector (Model R928P, Hamamatsu, Middlesex, NJ). Data at 1.0 cm^{-1} intervals were collected with an integration time of 1.5 s and a spectral slit width of 8 cm^{-1}. Samples were scanned repetitively, and individual scans were displayed and examined prior to averaging. The spectrometer wavenumber drive was calibrated using liquid indene. Frequencies cited are accurate to within ±1 cm^{-1} for sharp bands and up to ±2 cm^{-1} for very broad bands or shoulders. Further details of the instrumentation and data collection protocols are given elsewhere (Li et al., 1981; Aubrey & Thomas, 1991).

Raman spectra of different samples were compared by digital difference methods using SpectraCalc software (Galactic Inds., Salem, NH). Ordinarily, the difference spectra were computed prior to correcting the raw data for contributions of solvent and background. Advantages of this approach have been discussed (Aubrey & Thomas, 1991). For difference spectra shown in the figures, the spectrum of the deuterated or mutated virus was employed generally as the minuend and the spectrum of the normal or wild-type virus as the subtrahend.

RESULTS

Figure 3 compares the Raman spectrum in the 300−1800 cm^{-1} region of the native *Ff* virion (*fd*) with spectra of variants containing deuterated aromatic side chains [*fd*(3F$_{d5}$), *fd*(W$_{d5}$), and *fd*(2Y$_{d4}$)]. The bands diagnostic of the deuterium isotopomers appear as peaks in the difference spectra of Figure 3, while markers of the normal (non-deuterated) virion appear as troughs. Figure 4 displays spectra in the 2200−3150 cm^{-1} region of the same viruses. A comprehensive tabulation of the Raman frequencies of each *Ff* isotopomer is given in Table 1, and assignments are detailed in the Discussion section.

Figure 5 compares Raman spectra in the 600−900 and 1500−1800 cm^{-1} regions of *fd*(3F$_{d5}$) in native and thermally denatured forms.

Figure 6 compares the Raman spectrum in the 300−1800 cm^{-1} region of the wild-type *Ff* virion (*f1*) with spectra of tyrosine single mutants, *f1*(Y21M) and *f1*(Y24M), and a double mutant, *f1*(Y21F/Y24S). These data, complemented by spectra of Figure 5, provide definitive information on the tyrosine contributions to the *Ff* spectra. The significance of these results is considered in the Discussion section.

DISCUSSION

Raman Markers of the Aromatic Side Chains in Ff Subunits. (a) Residues F11, F42, and F45. Incorporation of F$_{d5}$ into pVIII alters many prominent Raman bands of *fd* in the spectral interval 300−1800 cm^{-1} (Figure 3). In the b − a difference spectrum of Figure 3, the *negative* bands (troughs) at 477, 620, 742, 754, 827, 1002, 1031, 1050, 1086, 1178, 1204, 1356, 1481, 1588, and 1606 cm^{-1} identify these frequencies as markers of the F11, F42, and F45 residues of pVIII, as assigned in Table 1. The bands at 620, 827, 1002, 1031, and 1605 cm^{-1} are due exclusively or predominantly to phenylalanine; all others contain overlapping contributions from bands of additional pVIII side chains or DNA nucleotide residues. The *positive* difference bands in the b − a spectrum of Figure 3 are those of the deuteriophenylalanyl side chains of *fd*(3F$_{d5}$), as assigned in Table 1.

In the 2200−3150 cm^{-1} interval (Figure 4), difference bands at 3064 and 3070 cm^{-1} are assigned on the basis of their respective deuteration shifts to 2273 and 2294 cm^{-1} to aromatic CH stretching modes of the phenyl ring.

Many of the peaks and troughs in the b − a difference spectra of Figures 3 and 4 correspond identically to bands in Raman spectra of the normal and deuterated amino acids (Figure 1 and additional data not shown). For example, we observe that the sharp band of *fd* at 1002 cm^{-1} is shifted to 960 cm^{-1} in *fd*(3F$_{d5}$) (Figure 3), and a virtually identical shift is observed between F and F$_{d5}$ (Figure 1). These results are consistent with previously reported spectra of the free amino acid [reviewed in Harada and Takeuchi (1986) and Austin et al. (1993)] and with normal coordinate analyses (Harada & Takeuchi, 1986). Additionally, the more comprehensive spectra reported here identify several previously unassigned modes as due to coupled phenyl ring stretching and CH in-plane bending or to coupled out-of-plane ring and CH deformation vibrations. Further, the high signal-to-noise quality of present spectral data allows identification of previously unreported phenylalanine bands, including those of *fd* at 477, 742, 754, 827, 1050, 1086, 1356, and 1481 cm^{-1}. All have obvious counterparts in the spectrum of the free amino acid (Figure 1), which supports their reliability as markers of phenylalanine. *Most important among these is the band of fd at 827 cm^{-1}.* This band is absent from the spectrum of *fd*(3F$_{d5}$), which establishes its assignment to phenylalanine side chains of the pVIII subunit. In other proteins and protein assemblies, a Raman band near 825−830 cm^{-1} is ordinarily assigned to tyrosine (Siamwiza et al., 1975). The significance of the assignment of the 827 cm^{-1} band of *fd* to F11, F42, and F45 residues, rather than to Y21 and Y24 residues of pVIII, has been noted recently (Overman et al., 1994). Further discussion is given below.

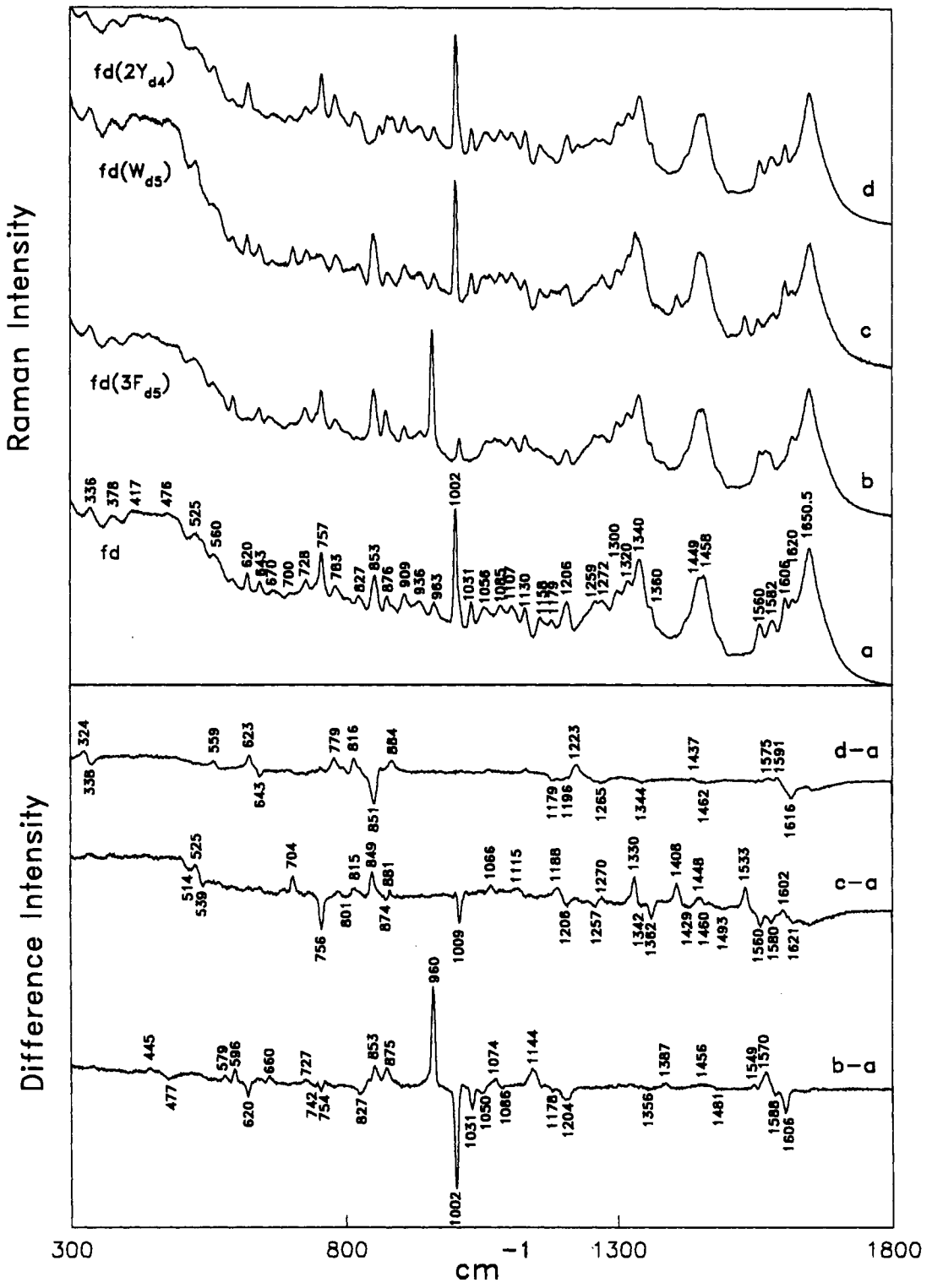

FIGURE 3: Upper panel: Raman spectra (300−1800 cm^{-1}) of unlabeled and isotopically labeled *fd* viruses. Sample concentrations are 80 mg/mL in 10 mM Tris at pH 7.8. Each spectrum is the average of eight scans. Lower panel: Normalized difference spectra, computed with the isotopically labeled virus as minuend and the unlabeled virus as subtrahend. Difference intensities (peaks and troughs) are normalized to approximate corresponding band intensities in the parent spectra. Other conditions are given in Figure 1.

Surprisingly, the 827 cm^{-1} Raman frequency has not been considered in previous normal coordinate calculations on phenylalanine (Harada & Takeuchi, 1986), even though it is ubiquitous among monosubstituted benzene derivatives (Lin-Vien et al., 1991). Earlier surveys attribute a Raman band near 650−850 cm^{-1} in monosubstituted benzenes to a coupled vibrational mode involving the so-called "quadrant in-plane bending" of the phenyl ring and stretching of the substituent exocyclic bond. The mode is sometimes designated by the symbol ν_1 (or *F1* in the present notation), by analogy with the hexagonal ring breathing mode of benzene (Lin-Vien et al., 1991; Colthup et al., 1990; Austin et al., 1993).

(b) Residue W26. Upon deuteration of the W26 indole ring of the viral subunit, many prominent Raman bands of *fd* shift to lower frequency, as seen in the c − a difference

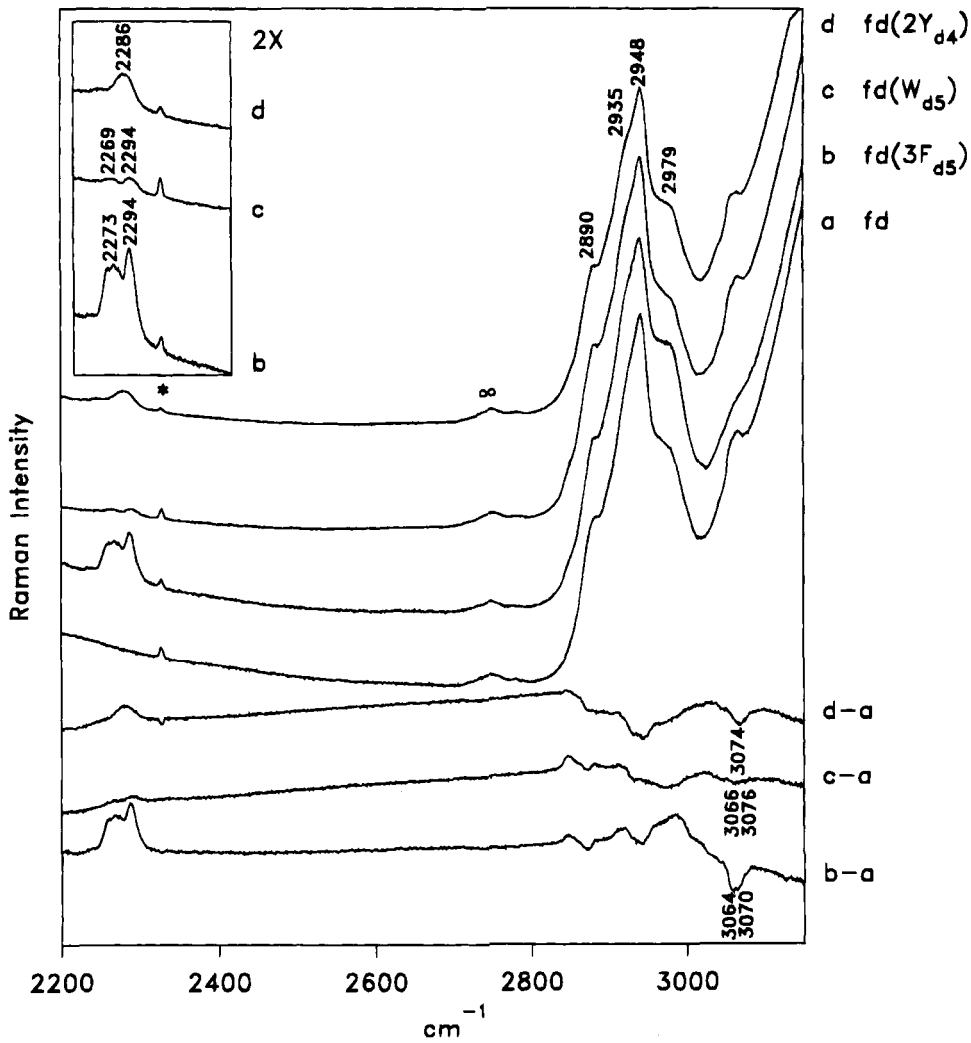

FIGURE 4: Raman spectra (2200−3150 cm^{-1}) of unlabeled (a) and isotopically labeled *fd* viruses (b, c, d). Each spectrum is the average of two scans. Also shown are normalized difference spectra (d − a, c − a, b − a), computed with the isotopically labeled virus as minuend and the unlabeled virus as subtrahend. The inset at upper left shows a 2-fold amplification of the CD stretching bands in spectra b, c, and d. Other conditions are given in Figure 3. The symbols * and ∞ indicate respectively Raman bands due to ambient N_2 (2331 cm^{-1}) and overtones.

spectrum of Figure 3. Each labeled trough in the difference spectrum corresponds to a frequency diagnostic of the W26 residue of pVIII. Although many of the tryptophan bands have been reported (Aubrey & Thomas, 1991), the present results identify new tryptophan markers at 801, 1257, 1429, 1460, 1493, and 1621 cm^{-1}, each of which is represented in the spectrum of the free amino acid (Figure 1). On the basis of correlations established by Miura et al. (1989), the 1429 and 1493 cm^{-1} bands confirm moderate hydrogen bonding of the indole N−H donor, consistent with previous analysis (Aubrey & Thomas, 1991).

In the 2200−3150 cm^{-1} interval (Figure 4), difference bands at 3066 and 3076 cm^{-1} are assigned, on the basis of their respective deuteration shifts to 2269 and 2294 cm^{-1}, to aromatic CH stretching modes of the indole ring.

(c) Residues Y21 and Y24. Incorporation of Y_{d4} into *fd* leads to troughs at 338, 643, 851, 1179, 1196, 1267, 1344, 1462, 1606 (shoulder), and 1616 cm^{-1} in the d − a difference spectrum of Figure 3, indicating contributions from Y21 and Y24. The markers at 643, 851, and 1616 cm^{-1} are due virtually exclusively to tyrosine, while the remaining markers are overlapped by Raman bands from other pVIII side chains or DNA (Table 1). The data shown for *fd* and *fd*($2Y_{d4}$) in Figure 3 are consistent with the spectra of Y and Y_{d4} (Figure 1) and with studies of the tyrosine model compound, *p*-cresol, and its deuterated analogues (Harada & Takeuchi, 1986; Takeuchi et al., 1988).

In the 2200−3150 cm^{-1} interval (Figure 4), the difference band at 3074 cm^{-1} is assigned, on the basis of its deuteration shift to 2286 cm^{-1}, to CH stretching of the para-substituted phenyl ring. The four aromatic hydrogens apparently contribute to the single broad band.

The superior signal-to-noise quality of the present *fd* spectra allows detection of many weak bands of pVIII tyrosines not reported previously. In particular, the new tyrosine markers at 338, 1344, and 1462 cm^{-1} in the d − a difference spectrum of Figure 3 amend earlier assignments (Thomas et al., 1983). Their designation as tyrosine markers is consistent with the spectrum of the free amino acid (Figure 1) and previous studies (Harada & Takeuchi, 1986; Takeuchi et al., 1988). We note also that the tyrosyl $\nu_{7a'}$ vibration (hereinafter, *Y7a'*), due mainly to phenoxyl C−O stretching, is expected in the 1255−1275 cm^{-1} interval. On the basis of the low-intensity trough centered near 1267 cm^{-1} (Figure 3, d − a), we assign *Y7a'* near this frequency for both of the tyrosines of pVIII. Although the Raman intensity of *Y7a'*

Table 1: Raman Frequencies and Assignments for Isotopomers of Filamentous Virus *fd*

fd[a]	assignment[b]	*fd*-($3F_{d5}$)	*fd*-(W_{d5})	*fd*-($2Y_{d4}$)	*fd*-($3F_{d5}$,W_{d5},$2Y_{d4}$)	*fd*[a]	assignment[b]	*fd*-($3F_{d5}$)	*fd*-(W_{d5})	*fd*-($2Y_{d4}$)	*fd*-($3F_{d5}$,W_{d5},$2Y_{d4}$)
	Y_{d4}			326	326		F_{d5}, W_{d5}	1069	1070		1069
336	Y	*c*	*c*			1085	CC str, bk, F	*d*	*c*	*c*	*d*
378	mc	*c*	*c*	*c*	*c*	1107	A	*c*	*c*	*c*	*c*
	Y_{d4}			387	387	1130	CC str, W	*c*	*d*	*c*	*d*
417	Y	*c*	*c*				F_{d5}	1142			1143
424	mc	*c*	*c*	*c*	*c*	1158	CC str	*c*	*c*	*c*	*c*
	F_{d5}	442			441	1179	Y, F	*d*	*c*	*d*	*d*
476	F		*c*	*c*			W_{d5}		1188		1187
493	Thy, Gua	*c*	*c*	*c*	*c*	1206	F, Y, W	*d*	*d*	*d*	*d*
	W_{d5}		527		527		Y_{d4}			1228	1224
525	mc	*c*	*c*	*c*	*c*		Y_{d4}			1242	1242
534	mc, W	*c*	*d*	*c*	*d*	1243	amIII, Thy, Cyt	*c*	*c*	*c*	*d*
	Y_{d4}			560	559		Y_{d4}			1257	1258
560	mc	*c*	*c*	*c*	*c*	1259	amIII, Thy, Ade, W	*c*	*d*	*c*	*d*
	F_{d5}	578			578	1272	amIII, Y	*c*	*c*	*d*	*d*
594	mc	*c*	*c*	*c*	*c*	1300	CH, CH_2 def	*c*	*c*	*c*	*c*
	F_{d5}	595			595	1320	CH_2 def	*c*	*c*	*c*	*c*
620	F		*c*	*c*	*d*		W_{d5}		1332		1330
	Y_{d4}			622	626	1340	CH_2, CH_3 def; W, Y	*c*	*d*	*d*	*d*
	-				634	1360	W, F	*d*	*d*	*c*	
643	Y	*c*	*c*		*d*		F_{d5}	1384			1387
	F_{d5}	660			659		W_{d5}		1408		1408
670	Thy, Gua	*c*	*c*	*c*	*c*	1431	CH_2, CH_3 def; W	*c*	*c*	*c*	*c*
	W_{d5}		685		685		Y_{d4}			1437	1437
700	-	*c*	*c*	*c*	*c*		W_{d5}		1449		1449
	W_{d5}		704		706	1449	CH_2, CH_3 def	*c*	*c*	*c*	*c*
728	Ade	*c*	*c*	*c*	*c*	1458	CH_2, CH_3 def; A, W, Y	*c*	*d*	*d*	*d*
746	Thy, F	*d*	*c*	*c*	*d*		F_{d5}	1456			1459
757	W, F	*d*		*c*			W_{d5}		1468		1468
	Y_{d4}			782	780	1483	Ade, Gua, W, F	*d*	*d*	*c*	*d*
783	Cyt	*c*	*c*	*c*	*c*		W_{d5}		1534		1533
806	bk, W	*c*	*d*	*c*	*d*		F_{d5}	1549			1558
	Y_{d4}			822	816	1560	W	*c*	*d*	*c*	*d*
	W_{d5}		817		816		F_{d5}	1571			1570
827	F		*c*	*c*			Y_{d4}			1578	1578
	F_{d5}	852			848	1582	W, F, Gua, Ade	*d*	*d*	*c*	*d*
853	Y	*c*	*c*		*d*		Y_{d4}			1591	1591
	F_{d5}	874			873	1606	F, Y	*d*	*c*	*d*	*d*
876	W	*c*		*c*	*d*	1620	Y, W	*c*	*d*	*d*	*d*
	Y_{d4}			887	882	1651	amI	*c*	*c*	*c*	*c*
885	-	*c*	*c*	*c*	*c*		W_{d5}		2269		2275
909	A	*c*	*c*	*c*	*c*		F_{d5}	2273			2275
936	CCC def	*c*	*c*	*c*	*c*		Y_{d4}			2286	2275
	F_{d5}	959			959		F_{d5}, W_{d5}	2294	2294		2292
963	-	*c*	*c*	*c*	*c*	2890	CH_3, CH_2, CH str	*d*	*d*	*d*	*d*
1002	F		*c*	*c*		2935	CH_3, CH_2, CH str	*d*	*d*	*d*	*d*
1010	W	*c*		*c*		2948	CH_3, CH_2, CH str	*d*	*d*	*d*	*d*
	Y_{d4}				1020	2979	CH_3, CH_2, CH str	*c*	*d*	*d*	*d*
1031	F, Y		*c*			3071	F, Y, W	*d*	*d*	*d*	*d*
1056	CC, CN, CO str; F	*d*	*c*	*c*	*d*						

[a] Raman frequencies, in cm^{-1}, are reproducible to within ± 1 cm^{-1} for well-resolved bands and ± 2 cm^{-1} for very weak bands or shoulders. A blank space signifies either that no band occurs in the spectrum or that a band, if present, is assigned to a residue other than the labeled aromatic. [b] Abbreviations and notation are as follows: 1-letter symbols are used for amino acids; 3-letter symbols are used for DNA bases; bk, DNA backbone; mc, pVIII main chain; amI, amide I; amIII, amide III; str, stretching; def, deformation; CH, methyne; CH_2, methylene; CH_3, methyl; CC, carbon−carbon bond; CN, carbon−nitrogen bond; CO, carbon−oxygen bond. A hyphen indicates that the assignment is presently unknown. Other notation is defined in the text. [c] The deuterated isotopomer exhibits the same Raman band frequency and intensity as normal *fd*. [d] The deuterated isotopomer exhibits the same Raman band frequency but a lower intensity.

is low in comparison to strong amide III bands of the 1250−1300 cm^{-1} interval, the Raman frequency is considered to be sensitive to the strength of hydrogen bonding of the phenoxyl OH donor (Takeuchi et al., 1989) (see below).

(d) Complete Substitution of Deuterated Aromatics. The Raman spectrum of the isotopomer *fd*($3F_{d5}$,W_{d5},$2Y_{d4}$), in which all of the aromatic amino acids of coat subunits have been deuterated, exhibits all of the features described in the three preceding sections. [The Raman spectrum of *fd*-($3F_{d5}$,W_{d5},$2Y_{d4}$) is available from the authors upon request.]

Absence of a Tyrosine Fermi Doublet in Raman Spectra of Ff Subunits. On the basis of model compound studies (Siamwiza et al., 1975; Takeuchi et al., 1988), all tyrosine-containing proteins are expected to display a pair of Raman bands near 850 and 830 cm^{-1} attributable to a Fermi doublet and diagnostic of phenolic OH hydrogen bonding. The hydrogen-bonding correlation of Siamwiza et al. (1975) is as follows: (i) When the phenolic OH group acts predominantly as the donor of a strong hydrogen bond to an electronegative acceptor, such as a carboxyl oxygen, the intensity ratio of the doublet, measured as I_{850}/I_{830}, achieves a minimum value of 0.30. (ii) When the phenolic OH group acts as both donor and acceptor of moderate hydrogen bonds, for example, when exposed to solvent H_2O molecules, I_{850}/

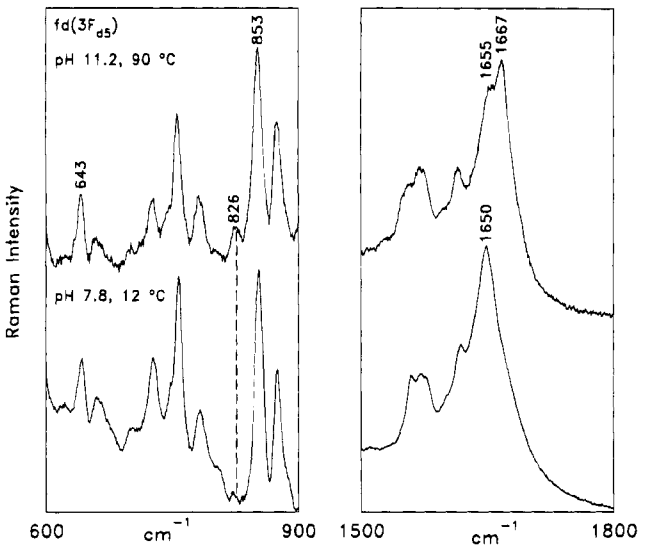

FIGURE 5: Raman spectra in the 600−900 (left) and 1500−1800 cm^{-1} (right) regions of *fd*(3F$_{d5}$) virus in native and partially denatured states. The native spectrum (lower traces) is from Figure 3. The denatured spectrum was obtained from a sample brought to pH 11.2 and maintained at 90 °C while data were collected. Other conditions are given in Figure 1.

$I_{830} = 1.25$. (iii) When the phenolic OH group acts as the acceptor of a strong hydrogen bond from an electropositive donor, such as a lysyl NH_3^+ group, and does not participate in significant hydrogen bond donation, then I_{850}/I_{830} achieves a presumed maximum value of 2.50. (iv) Finally, when tyrosine is deprotonated at elevated pH to form the phenoxide ion, then $I_{850}/I_{830} \approx 0.70$.

Conspicuous by its absence from trace d − a of Figure 3 is any indication of a tyrosine band near 830 cm^{-1}; *i.e., tyrosines Y21 and Y24 of pVIII do not exhibit the canonical Fermi doublet.* Our results show, unexpectedly, that phenylalanines F11, F42, and F45 are the sole contributors (827-cm^{-1} band) to this region of the *fd* Raman spectrum. Residues Y21 and Y24 of pVIII thus violate the correlation of Siamwiza et al. by exhibiting a Raman *singlet* at 853 cm^{-1}. The basic requirement for the tyrosine Fermi doublet, namely, the accidental degeneracy or near degeneracy of a fundamental and an overtone of the same symmetry species, is apparently not fulfilled for either Y21 or Y24 in viral subunits. We have attributed this anomaly to unusual local environments of these side chains in native *Ff* virions (Overman et al., 1994).

The tyrosine singlet assignment at 853 cm^{-1} rests ultimately upon the exclusivity of isotope labeling of phenylalanines in *fd*(3F$_{d5}$). To ensure that host cells produced only *fd*(3F$_{d5}$) when infected in media containing F$_{d5}$ as the only labeled amino acid source, we employed a tyrosine auxotrophic host (*E. coli* strain AT2471, courtesy of Prof. Barbara Bachman, Yale University) for production of *fd*(3F$_{d5}$). Additionally, *fd*(3F$_{d5}$) was grown in media containing a large excess of normal tyrosine. In both cases, the virions yielded a Raman spectrum identical to that of Figure 3, trace b. Therefore, metabolic conversion of deuterated phenylalanine to deuterated tyrosine does not occur in these experiments. Accordingly, spectrum b of Figure 3 is assigned unambiguously to virions containing deuterated phenylalanine and normal tyrosine residues.

In further confirmation of the tyrosine singlet assignment for native *fd*, we obtained Raman spectra of partially denatured virus particles generated by heat treatment at elevated pH. Our expectation was that virion disassembly would lead to solvent exposure of at least some subunit tyrosines, thus generating for the exposed residues a more typical tyrosine Fermi doublet. Denaturation of the phage is verified independently by the shift of Raman amide I from 1650 cm^{-1} (α-helix) to 1667 cm^{-1} (β-strand). The results, shown in Figure 5, indicate that loss of native virus structure generates a distinctive Raman marker at 827 cm^{-1} assignable to the otherwise missing low-frequency component of the tyrosine Fermi doublet. This experiment is consistent with the notion that tyrosines of *fd* are characterized by a Raman singlet at 853 cm^{-1}. Thermal disruption of the native virion architecture is sufficient to generate a normal tyrosine Fermi doublet. Figure 5 also implies that the anomalous Raman singlets for Y21 and Y24 in the native virion state do not result from covalent modifications of these tyrosine residues.

Finally, we note that the present deuteration results are entirely consistent with previously reported Raman spectra of mutant variants of *Ff* (Overman et al., 1994). In the single-site mutants *f1*(Y21M) and *f1*(Y24M), the 827 cm^{-1} band intensity is not affected, while the 853 cm^{-1} band intensity is diminished by roughly one-half in comparison to wild type. In the double mutant *f1*(Y21F/Y24S), the 827 cm^{-1} band reflects only the additional F21 residue, while the 853 cm^{-1} band is essentially eliminated. Thus, both site-specific mutagenesis and residue-specific deuteration studies (summarized graphically in Figure 7) support the assignment of a singlet at 853 cm^{-1}, rather than a doublet, to tyrosines Y21 and Y24 of pVIII. In the next section we discuss more comprehensive spectral assignments for *Ff* mutants and their structural significance.

Structural Significance of Raman Spectra of Mutant Ff Virions. Raman spectra of the mutant virions *f1*(Y21M), *f1*(Y24M), and *f1*(Y21F/Y24S) (Figure 6) provide independent confirmation of the tyrosine assignments deduced from the above noted deuteration effects (Figure 3, trace d − a, and Table 1). Specifically, the spectra of *f1*(Y21M) and *f1*(Y24M) reveal, respectively, that residues Y21 and Y24 contribute only to the band near 853 cm^{-1} and not to the band near 827 cm^{-1}; i.e., in the mutant virions, as well as in the wild-type virion, each subunit tyrosine lacks a Fermi doublet in the 820−860 cm^{-1} region of the Raman spectrum.

We have also computed Raman difference spectra [*f1*(Y21M) − *fd* and *f1*(Y24M) − *fd*] to locate markers of each tyrosine separately. To a first approximation, the difference spectrum *f1*(Y21M) − *fd* should yield negative difference bands diagnostic of Y21 in the wild-type *fd* spectrum. Similarly, *f1*(Y24M) − *fd* should approximate the markers of Y24. The computed difference spectra (Figure 6, bottom, and Table 2, top) show that in this approximation Y21 and Y24 of *fd* exhibit distinctly different Raman markers, not only near 853 cm^{-1} but also in the 1175−1280 cm^{-1} interval. Particularly interesting are the bands related to vibrational normal modes *Y7a* and *Y7a′* (Takeuchi et al., 1989). Thus, Y21 exhibits markers at 1193, 1211, and 1268 cm^{-1}; the first two bands appear to be related to vibrational mode *Y7a*, and the last, to *Y7a′*. For Y24, on the other hand, the markers occur at 1203 (*Y7a*) and 1261 cm^{-1} (*Y7a′*). Takeuchi et al. (1989) have discussed the sensitivity of Raman bands of this region to hydrogen-bonding interactions of phenol derivatives in various solvents. However, in view of the absence of a canonical Fermi doublet (830/850 cm^{-1})

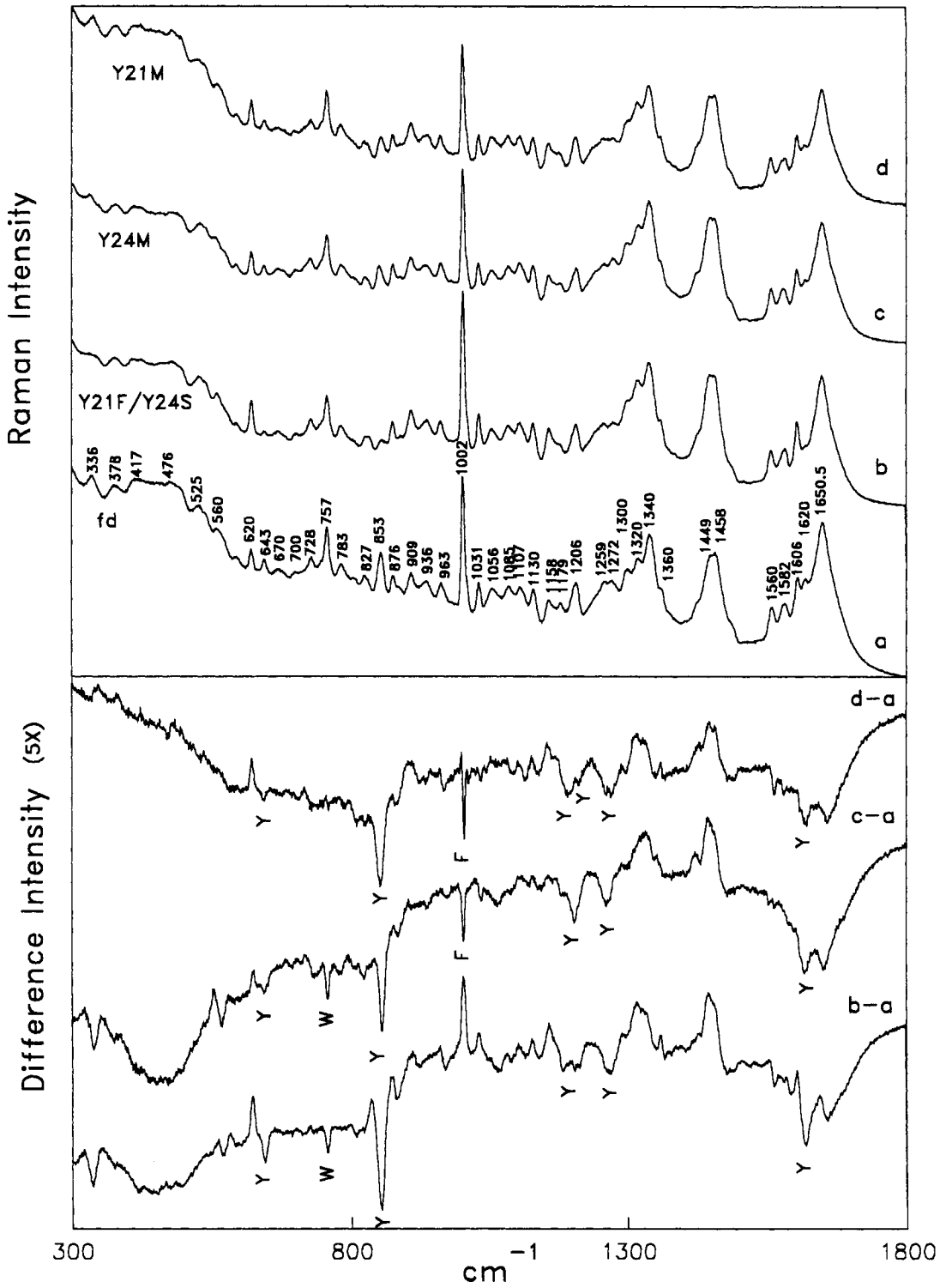

FIGURE 6: Upper panel: Raman spectra in the 300−1800 cm^{-1} region of wild-type and mutant *f1* viruses. Sample concentration is 80 mg/mL in 10 mM Tris at pH 7.8. Each spectrum is the average of eight scans. No smoothing or solvent corrections were employed. Lower panel: Normalized difference spectra, computed with the mutant virus as minuend and the wild-type virus as subtrahend. Difference intensities (peaks and troughs) were normalized to approximate the corresponding band intensities in the parent spectra.

for both tyrosines of *Ff* viruses, previously developed correlations for bands of the 1175−1280 cm^{-1} interval may not be fully applicable. In summary, the present results provide indirect evidence that the side chains of Y21 and Y24 in the native virus are not equivalent, even though both share the distinguishing characteristic of a singlet rather than a Fermi doublet in the 820−860 cm^{-1} interval of the Raman spectrum. The tyrosine assignments indicated by the spectra of *Ff* mutants are listed in Table 2.

Figure 6 shows that the Raman spectrum of the double mutant *f1*(Y21F/Y24S) contains weak bands near 339, 643, and 1619 cm^{-1}. Since no other pVIII side chains contribute at these spectral positions, these residual intensities are attributed to tyrosines. The bands are far too weak to arise from the stoichiometric equivalent of one tyrosine per coat subunit and can be attributed to minor contamination of the double mutant with a genetic revertant containing tyrosine. A revertant is confirmed by genetic experiments (G. Ce-

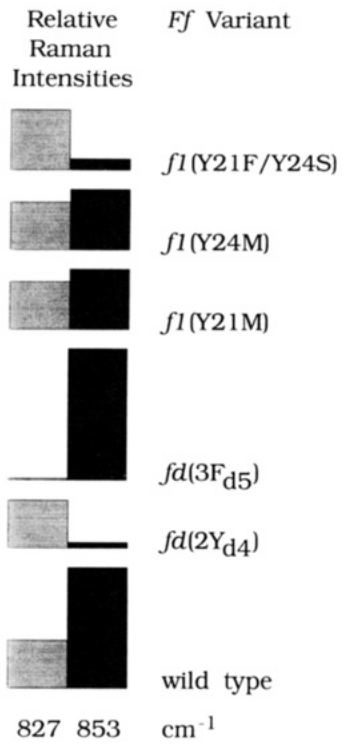

FIGURE 7: Schematic representation of relative Raman intensities of bands observed at 827 ± 1 and 853 ± 1 cm^{-1} in spectra of *Ff* variants listed in the right column. The figure illustrates the invariance of the 827 cm^{-1} band intensity and the sensitivity of the 853 cm^{-1} band intensity to deuterations or mutations of tyrosine. Conversely, phenylalanine perturbations affect the band at 827 cm^{-1}.

sareni, private communication). The Raman markers of the *f1*(Y21F/Y24S) variant are thus consistent with the data obtained from single-mutant and wild-type virions.

In addition to the foregoing changes in tyrosine marker bands, the mutation of Y24 produces a significant change in the intensity of the 757 cm^{-1} band of the subunit tryptophan residue (W26), as indicated in Figure 6. The band in question, assigned to indole mode *W18*, is clearly weaker in *f1*(Y24M) and *f1*(Y21F/Y24S) than in virions containing Y24. Intensity loss in the 757 cm^{-1} band has been correlated with increasingly hydrophobic interactions of the indole ring (Miura et al., 1991). The present data indicate more strongly hydrophobic interactions of W26 when Y24 is mutated to M. This suggests that W26 interacts either directly or indirectly with Y24 in the wild-type virion. On the other hand, the tryptophan band near 1560 cm^{-1} (mode *W3*, diagnostic of side-chain torsion $X^{2,1}$) (Miura et al., 1989) is not significantly affected by the tyrosine mutations. Similarly, the *W17* mode occurs near 880 cm^{-1} in all mutants, indicating that the indole N−H group remains a weak hydrogen bond donor (Miura et al., 1988), irrespective of the tyrosine mutations.

Figure 6 shows that the band at 1002 cm^{-1}, assigned to the symmetrical phenyl ring stretching mode (*F12*) of subunit phenylalanines (F11, F42, and F45), is also sensitive to tyrosine mutations. Each of the single mutations reduces the intensity vis-à-vis wild type. Although the relationship of the 1002 cm^{-1} band to the phenyl ring environment is not known, it has been speculated that the intensity is sensitive to phenyl ring interactions (Thomas et al., 1983; Grygon et al., 1988). In the absence of a more detailed understanding of the Raman intensity, we can infer only that each tyrosine influences in some manner the environment of one or more of the phenylalanyl side chains.

Finally, Figure 6 shows that bands assignable to CH deformation modes of aliphatic side chains (ca. 1316, 1330, 1445, and 1458 cm^{-1}) are systematically more intense in mutants than in wild-type *fd*. Although specific spectra−structure correlations are not available for these bands, the present data indicate that aliphatic as well as aromatic side chains are influenced by the tyrosine mutations. This is consistent with the expectation that substitution of a less bulky side chain (methionine or serine) for a tyrosine would introduce some rearrangement of local structure to conserve close packing of pVIII subunits in the *Ff* assembly.

SUMMARY AND CONCLUSIONS

In this work we have incorporated deuteriophenylalanine, deuteriotryptophan, and deuteriotyrosine side chains, singly and in combination, into pVIII subunits of the native *Ff* filamentous virion. Spectra obtained from these *Ff* deuterioisotopomers permit definitive assignment of all prominent Raman bands contributed by phenylalanine (F11, F42, F45), tryptophan (W26), and tyrosine (Y21, Y24) residues in the native virus structure. Additionally, many weaker Raman bands of *Ff* have been identified as originating in whole or in part from specific aromatic side chains of the coat subunits. The overall assignment scheme deduced from the data (Table 1) defines a more detailed fingerprint of aromatic amino acid environment than heretofore has been available for coat proteins of filamentous viruses. The present findings should be applicable generally to the problem of elucidating aromatic residue environments in proteins by Raman spectroscopy.

An important conclusion reached from the present study is that coat protein *phenylalanines*, rather than tyrosines, generate the prominent Raman band at 827 cm^{-1}. This phenylalanine assignment is novel for protein Raman spectroscopy and signifies a departure from the long-held view that such a band should be assigned categorically as an indicator of tyrosine phenoxyl hydrogen bonding (Siamwiza et al., 1975). The present results show not only that the 827 cm^{-1} band of *Ff* is due to phenylalanines of the pVIII subunits but also that the tyrosines make no spectral contribution within the 820−840 cm^{-1} interval. The tyrosines of *Ff* subunits thus lack the canonical Fermi doublet that is present in Raman spectra of other proteins. Both Y21 and Y24 are represented in the Raman spectrum of *Ff* by a single band near 853 cm^{-1}. While this tyrosine singlet assignment is reached conclusively from spectra of isotopically modified *Ff* viruses presented here, it is demonstrated independently by Raman signatures of mutant *Ff* virions which lack Y21 or Y24 (Overman et al., 1994).

The coupling of intensities of Raman bands due to subunit tyrosines, phenylalanines, and tryptophan, which is clearly manifested in the difference spectra of Figure 6, provides evidence that environments of these aromatic side chains within the native virion are strongly interdependent. Specifically, the Y21M mutation attenuates the intensity of the phenylalanyl ring marker at 1002 cm^{-1}, indicating that the environment of the Y21 side chain is somehow coupled with side-chain environments of one or more of the residues F11, F42, and F45. The same is true for coupling between F residues and Y24. The nature of the Raman perturbation suggests that phenylalanines may interact more strongly with

Table 2: Raman Markers for Residues Y21 and Y24 in *Ff* Virions[a]

Spectrum of wild-type *fd*	difference spectrum: *f1*(Y21M) − *fd*	difference spectrum: *f1*(Y24M) − *fd*	normal mode designation	comments
853	852	855	*Y1*	Singlet; a canonical Fermi doublet ({*Y1*/ 2*Y16a*}) is not observed for either Y21 or Y24.
	{1193/1211}		{*Y7a*/*Y13*+*Y6a*}	Proposed Fermi doublet for Y21.
		1203	*Y7a*	Singlet; a Fermi doublet ({*Y7a*/*Y13*+*Y6a*}) is not observed for Y24.
1206				Composite of Fermi doublet ({*Y7a*/*Y13*+*Y6a*}) for Y21 and singlet (*Y7a*) for Y24.
1265	1268	1261	*Y7a′*	May reflect different environments of Y21 and Y24.

[a] Table entries are Raman frequencies in cm^{-1} observed in spectra of the wild-type virion (column 1) or in the indicated difference spectra between mutant and wild-type (columns 2 and 3), as shown in Figure 6. Nomenclature for normal modes (column 4) is that of Harada and Takeuchi (1986).

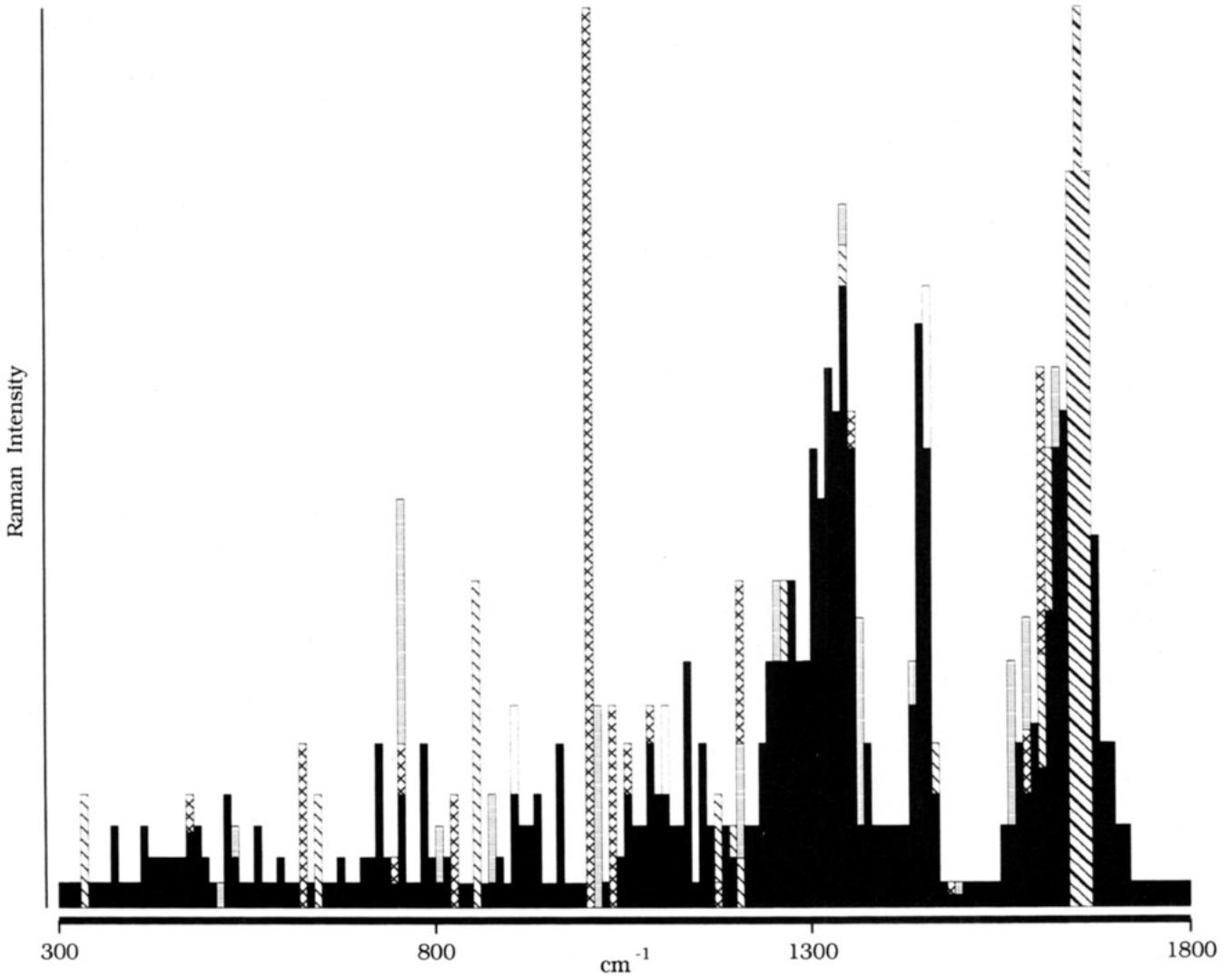

FIGURE 8: A representation of the Raman spectrum of the filamentous virus *Ff* which depicts definitive coat protein assignments determined by deuterium labeling of specific amino acid side chains. Present aromatic assignments are indicated by cross-hatching (phenylalanine), stippling (tryptophan), and thin hatching (tyrosine). Alanine assignments of Aubrey and Thomas (1991) are indicated by open bars. Alternating (thick/thin) hatch marks represent the amide I band. Bands which remain to be assigned definitively are represented as filled rectangles. [Tentative assignments for many of these bands have been proposed. See Thomas et al. (1983, 1988).]

one another in the absence of either Y21 or Y24. Our results indicate further that mutation of Y24 alters the hydropathicity of the W26 indole ring environment without affecting the strength of indole NH hydrogen bonding. The implication is that the side chains of Y24 and W26 are also structurally coupled, though not through a direct hydrogen-bonding interaction. Interaction of Y24 with W26 may also affect participation of the indole ring in hydrophobic clustering with residues F11, Y21, F42, and F45. The present results do not discriminate intersubunit from intrasubunit interactions.

The unusual Raman singlet near 853 cm^{-1} exhibited by both Y21 and Y24 (Table 2) requires the integrity of subunit packing in the mature *Ff* virion. This is demonstrated by thermal denaturation of the native assembly, which leads to the emergence of a tyrosine Fermi doublet in the Raman spectrum (Figure 5). Since the spectral change requires highly elevated temperature (90 °C) and pH (11.2), we conclude that the proposed structural coupling among

aromatic side chains of packed subunits is extraordinarily thermostable.

Recently described molecular models for the *Ff* virion may be examined for consistency with the present spectroscopic results. According to the model of Marvin and co-workers (Marvin et al., 1994), three phenylalanines, two tyrosines, and a single tryptophan from four neighboring subunits are positioned in such a manner that the seven aromatics form an extended array. The asymmetric unit defined by this array comprises F11 from one polypeptide chain, W26 from a second chain, Y21 and Y24 from a third chain, and F42 and F45 from a fourth chain. Such a model is essentially consistent with the Raman data. Additionally, we find that W26 is less influenced by Y21 than by Y24, suggesting that the latter is the tyrosine more likely to interact directly with the indole residue in the putative aromatic cluster. The model of Glucksman et al. (Glucksman et al., 1992), which does not address pVIII aromatic environments in detail, concludes that fiber X-ray diffraction data favor the positioning of Y21 and Y24 of a given subunit on opposing faces of an α-helical wheel. This interpretation would appear to be less consistent with an assembly in which both phenoxyl residues participate in clustering with phenylalanine and tryptophan side chains.

The Y21M and Y24M mutations also generate striking changes in the strong Raman bands near 1350 and 1450 cm^{-1} (Figure 6). This implies that many nonaromatic side-chain environments are likewise coupled with that of tyrosine. At present, the identities of the perturbed nonaromatic residues are not known. In Figure 8 we show schematically the frequency and intensity distributions of Raman bands which are presently assigned to specific molecular subgroups of the *Ff* virion, as well as those which remain to be assigned. Future work will focus on identifying subunit side chains that are major contributors to the unassigned Raman bands. Comprehensive assignment of coat protein Raman bands in the *Ff* spectrum will serve to identify Raman markers anticipated for the packaged genome. The latter have the potential to provide information about the configuration of the single-stranded DNA chain and possible interactions of nucleotides with the protein coat.

REFERENCES

Arnold, G. E., Day, L. A., & Dunker, A. K. (1992) *Biochemistry 31*, 7984−7956.

Aubrey, K. L., & Thomas, G. J., Jr. (1991) *Biophys. J. 60*, 1337−1349.

Austin, J. C., Jordan, T., & Spiro, T. G. (1993) in *Biomolecular Spectroscopy*, (Clark, R. J. H., & Hester, R. E., Eds.) Part A, pp 55−127, Wiley, London.

Clack, B. A., & Gray, D. M. (1989) *Biopolymers 28*, 1861−1873.

Colthup, N. B., Daly, L. H., & Wiberley, S. E. (1990) *Introduction to Infrared and Raman Spectroscopy*, 3rd ed., Academic Press, London.

Cross, T. A., Tsang, P., & Opella, S. J. (1983) *Biochemistry 22*, 721−726.

Denhardt, D. T., Dressler, D., & Ray, D. S., Eds. (1978) *The Single Stranded DNA Phages*, Cold Spring Harbor Laboratory Press, Cold Spring Harbor, NY.

Gall, C. M., Cross, T. A., DiVerdi, J. A., & Opella, S. J. (1982) *Proc. Natl. Acad. Sci. U.S.A. 79*, 101−105.

Glucksman, M. J., Bhattacharjee, S., & Makowski, L. (1992) *J. Mol. Biol. 226*, 455−470.

Grygon, C. A., Perno, J. R., Fodor, S. P. A., & Spiro, T. G. (1988) *BioTechniques 6*, 50−57.

Harada, I., & Takeuchi, H. (1986) in *Spectroscopy of Biological Systems* (Clark, R. J. H., & Hester, R. E., Eds.) pp 113−175, Wiley, London.

Harada, I., Miura, T., & Takeuchi, H. (1986) *Spectrochim. Acta 42A*, 307−312.

Li, Y., Thomas, G. J., Jr., Fuller, M., & King, J. (1981) *Prog. Clin. Biol. Res. 64*, 271−283.

Lin-Vien, D., Colthup, N. B., Fately, W. G, & Grasselli, J. G. (1991) *The Handbook of Infrared and Raman Characteristic Frequencies of Organic Molecules*, Academic Press, London.

Marvin, D. (1989) *Int. J. Biol. Macromol. 11*, 159−164.

Marvin, D. (1990) *Int. J. Biol. Macromol. 12*, 125−138.

Marvin, D. A., Hale, R. D., Nave, C., & Citterich, M. H. (1994) *J. Mol. Biol. 235*, 260−286.

McDonnell, P. A., Shon, K., Kim, Y., & Opella, S. J. (1993) *J. Mol. Biol. 233*, 447−463.

Miura, T., & Thomas, G. J., Jr. (1994) in *Subcellular Biochemistry, Vol. 24, Proteins: Structure, Function, and Engineering* (Biswas, B. B., & Roy, S., Eds.) pp 55−99, Plenum, New York.

Miura, T., Takeuchi, H., & Harada, I. (1988) *Biochemistry 27*, 88−94.

Miura, T., Takeuchi, H., & Harada, I. (1989) *J. Raman Spectrosc. 20*, 667−671.

Miura, T., Takeuchi, H., & Harada, I. (1991) *Biochemistry 30*, 6074−6080.

Model, P., & Russel, M. (1988) in *The Bacteriophages* (Calendar, R., Ed.) Vol. 2, pp 375−456, Plenum, NewYork.

Nambudripad, R., Stark, W., Opella, S. J., & Makowski, L. (1991) *Science 252*, 1305−1308.

Opella, S. J., & McDonnell, P. A. (1993) in *NMR of Proteins* (Gronenborn, A. M., & Clore, G. M., Eds.) pp 159−189, CRC Press, Boca Raton, FL.

Overman, S. A., Aubrey, K. L., Vispo, N. S., Cesareni, G., & Thomas, G. J., Jr. (1994) *Biochemistry 33*, 1037−1042.

Russel, M. (1991) *Mol. Microbiol. 5*, 1607−1613.

Shon, K., Kim, Y., Colnago, L. A., & Opella, S. J. (1991) *Science 252*, 1303−1305.

Siamwiza, M. N., Lord, R. C., Chen, M. C., Takamatsu, T., Harada, I., Matsuura, H., & Shimanouchi, T. (1975) *Biochemistry 14*, 4870−4876.

Takeuchi, H., Watanabe, N., & Harada, I. (1988) *Spectrochim. Acta 44A*, 749−761.

Takeuchi, H., Watanabe, N., Satoh, Y., & Harada, I. (1989) *J. Raman Spectrosc. 20*, 233−237.

Taylor, A. L., & Trotter, C. D. (1967) *Bacteriol. Rev. 31*, 332−353.

Thomas, G. J., Jr., & Barlyski, J. R. (1970) *Appl. Spectrosc. 24*, 463−464.

Thomas, G. J., Jr., & Murphy, P. (1975) *Science 188*, 1205−1207.

Thomas, G. J., Jr., Prescott, B., & Day, L. A. (1983) *J. Mol. Biol. 165*, 321−356.

Thomas, G. J., Jr., Prescott, B., Opella, S. J., & Day, L. A. (1988) *Biochemistry 27*, 4350−4357.

Webster, R. E., & Lopez, J. (1985) in *Virus Structure and Assembly* (Casjens, S., Ed.) pp 235−267, Jones and Bartlett, Boston.

BI942764V